

## The chlorination kinetics of beneficiated ilmenite particles by CO+Cl<sub>2</sub> mixtures

H.Y. Sohn<sup>\*</sup>, L. Zhou<sup>1</sup>

Department of Metallurgical Engineering and of Chemical and Fuels Engineering, University of Utah, Salt Lake City, UT 84112-0114, USA

Received 21 April 1998; received in revised form 22 September 1998; accepted 5 October 1998

### Abstract

The chlorination kinetics of beneficiated ilmenite particles using carbon monoxide as the reducing agent were studied in a shallow fluidized bed. The effects of temperature, carbon monoxide and chlorine partial pressures, and particle size were determined in the absence of mass- and heat-transfer influences. The kinetics can be represented by the following equation in the 1173–1323 K range and within the ranges of other experimental conditions used in this work:

$$\lambda[\exp(X/\lambda) - 1] - b = 69.0 \exp(-18800/T) p_{\text{CO}}^{0.82} p_{\text{Cl}_2}^{1.05} t$$

where  $X$  is the fractional conversion,  $T$  the temperature in K,  $p$  the partial pressure in kPa, and  $t$  the time in min;  $b$  and  $\lambda$  are given by

$$b = 3.32 d_p^{-0.8} \quad (d_p \text{ in } \mu\text{m})$$

and

$$1/\lambda = 1.32 \times 10^3 d_p^{0.36} \exp(-11700/T) \quad (d_p \text{ in } \mu\text{m})$$

The results of this study on the chlorination kinetics of beneficiated ilmenite would be useful when evaluating the performance of TiCl<sub>4</sub> production using beneficiated ilmenite as a raw material. It is shown in this study that the chlorination kinetics of beneficiated ilmenite are quite different from those of natural rutile, for which most previous chlorination studies were made. © 1999 Elsevier Science S.A. All rights reserved.

**Keywords:** Chlorination; Kinetics; Beneficiated ilmenite particles

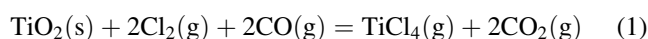
### 1. Introduction

With the special properties, such as high strength-to-density ratio and high corrosion and erosion resistances, titanium metal and alloys are attracting much attention [1,2]. Titanium dioxide is widely used in the paper, plastics, painting, and fabric industries [3,4].

With a diminishing reserve of natural rutile and an increasing demand for titanium and titanium products, beneficiated ilmenite has become an important raw material in the production of titanium tetrachloride [5], an intermediate for the production of titanium metal and pigment. However, there has been no published

information on the chlorination kinetics of beneficiated ilmenite.

Beneficiated ilmenite is a porous material, which is different from natural rutile, and is thus expected to have different chlorination kinetics. The kinetics of chlorination of rutile by CO–Cl<sub>2</sub> mixtures can be found in the literature [6–8]. The sample used in this work was obtained by removing the iron-oxide component from ilmenite by a process described below in Section 2. The chemical reaction involved in the removal of iron and oxygen creates titanium dioxide much different from natural rutile. The microstructure of beneficiated ilmenite and its changes during chlorination can be found elsewhere [9]. In this work, the intrinsic kinetics of chlorination of beneficiated ilmenite was investigated in a shallow fluidized bed to eliminate the mass- and heat-transfer effects. The overall chlorination reaction is



<sup>\*</sup>Corresponding author. Fax: +1-801-581-4937; e-mail: hysohn@mines.utah.edu

<sup>1</sup>Currently with Millenium Inorganic Chemicals, Baltimore, Maryland, 21226–1899.

## 2. Experimental work

Experiments were conducted to determine the effects of the original particle size, partial pressures of CO and Cl<sub>2</sub>, and temperature on the chlorination rate. The average original particle size of beneficiated ilmenite varied from 63 to 252 μm. Partial pressures of CO and Cl<sub>2</sub> changed from 9.6 to 57.4 kPa. The reaction temperature ranged from 900° to 1050°C. The total flow rate of the gas mixture was fixed at 900 cm<sup>3</sup>/min at 25°C and 86.1 kPa.

To avoid the photosynthesis of phosgene and prolong the life of Tygon tubing, all tubing carrying chlorine was shrouded with a black tape.

### 2.1. Sample preparation

The beneficiated ilmenite used in this experiment, provided by Du Pont, was produced in a two-stage process in which iron oxides in the ilmenite were reduced with coke at 1150°C to give metallic iron and titanium oxides. The reduced ilmenite was then agitated in aerated water in the presence of NH<sub>4</sub>Cl as a catalyst so that accelerated rusting of iron away from the ilmenite grain took place and the precipitated iron oxide was easily separated from the high TiO<sub>2</sub>-content product by decantation. The sample used in this work contained 92% TiO<sub>2</sub>, 4% iron oxide, and ca. 1% each of alumina, silica, and magnesium oxide.

### 2.2. Experimental apparatus and procedure

The experimental apparatus and procedure used in this work were the same as those used in the previous study of rutile chlorination [6,10]. The fluidized-bed reactor consisted of a quartz tube of 2.5 cm ID having a 5-cm ID expansion zone on top to reduce particle carry over. The total length was 95 cm and a coarse fritted disk served as the gas distributor and bed support. The titanium material balance was closed by analyzing the titanium chloride collected in a scrubber and the unreacted titanium dioxide left in the bed. Other details can be found in Refs. [6,10].

## 3. Results and discussion

When the reactant solid is porous, diffusion and chemical reaction occur simultaneously within the porous solid. The controlling step depends on the nature of the reaction and the structure of the materials.

### 3.1. Effect of flow rate

The effect of mass and heat transfer can be eliminated by using a shallow fluidized bed [11]. A flow rate of 900 cm<sup>3</sup>/min (25°C and 86 kPa) was found sufficient in this work, which is ca. 10 times higher than the minimum fluidization velocity.

### 3.2. Effect of particle size

Experiments to determine the effect of original particle size were conducted at 900°C by varying the average particle size from 63 to 252 μm in five fractions. The partial pressures of chlorine and carbon monoxide were kept at 43 kPa. The amount of titanium chlorinated at a given time increased with decreasing particle size, although the effect is not so large as with natural rutile. The small dependence on superficial particle size is due to the presence of porosity.

The shrinking-core model is not applicable in this case, because the sample is porous and thus pore diffusion occurs simultaneously with chemical reaction inside the particle, which does not allow a topochemical reaction. After several other rate expressions were tested to fit the experimental data, the following pore-blocking rate law was found to give the most satisfactory correlation of the results:

$$k_{app}t = \lambda[\exp(X/\lambda) - 1] \quad (2)$$

where  $X$  is the fractional conversion of titanium dioxide, and  $k_{app}$  and  $\lambda$  constants, independent of conversion. The constant  $\lambda$  is related to pore blockage which inhibits the access of reactant gases. This is likely to be due to the formation of high-boiling point liquid-phase materials such as ferrous chloride [11,12], or the structural changes of solid reactant during the chlorination reaction as documented previously [9]. The apparent rate constant,  $k_{app}$ , is a function of the partial pressures of reactant gases. Using a curve-fitting program, Sigma Plot [13], proper values of  $k$  and  $\lambda$  were obtained for various particle sizes. Fig. 1 shows the plot of the conversion function,  $\lambda[\exp(X/\lambda) - 1]$  vs. time for different particle sizes. The parallel lines in Fig. 1 indicate that  $k_{app}$  is a constant, indicating that  $k_{app}$  does not depend on particle size. Although straight lines were obtained, the lines

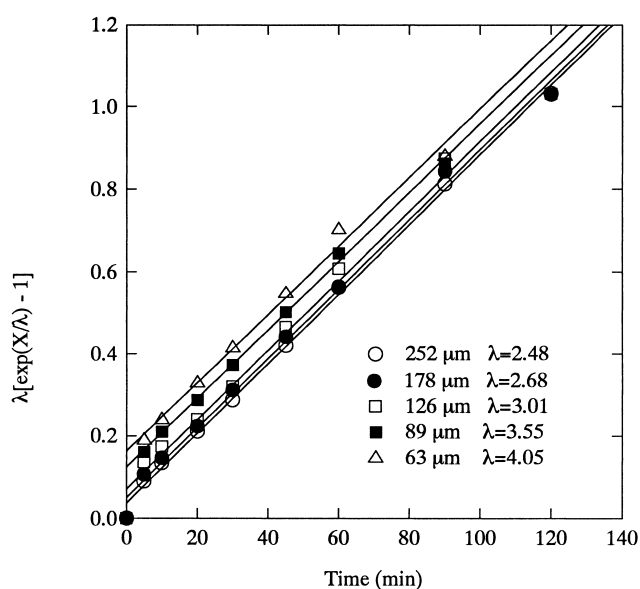


Fig. 1. Effect of particle size on the chlorination of beneficiated ilmenite ( $T=900^{\circ}\text{C}$ ;  $p_{\text{CO}}=p_{\text{Cl}_2}=43$  kPa).

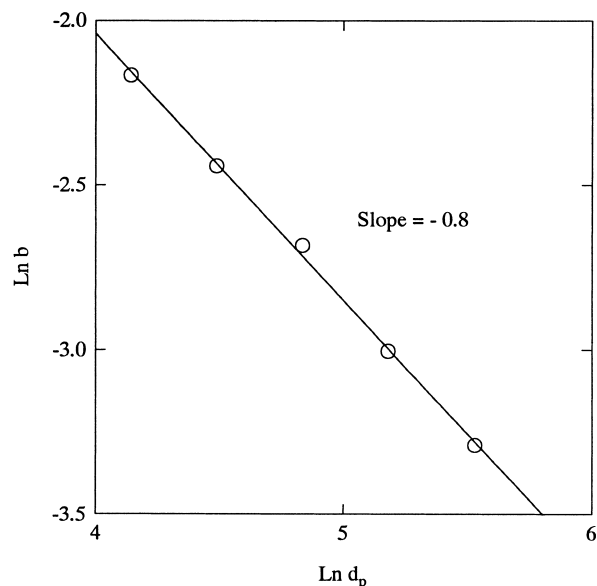


Fig. 2. Intercept in Fig. 1 vs. particle size ( $d_p$  in  $\mu\text{m}$ ).

do not exactly go through the origin. The small positive intercept with the vertical axis indicates that there is some rapid chlorination of the solid. This is likely to be due to the rapid chlorination of titanium dioxide on the external surface before the pore-blocking mechanism sets in. The intercept, designed as 'b', varied with particle size, as seen in Fig. 2. Their relationship can be expressed as:

$$b = 3.32d_p^{-0.8} \quad (d_p \text{ in } \mu\text{m}) \quad (3)$$

The relationship between  $\lambda$  and the original average particle diameter of beneficiated ilmenite,  $d_p$ , was derived by plotting  $\ln \lambda$  vs.  $\ln d_p$ , which yielded a straight line with a slope of  $-0.36$ , as can be seen from Fig. 3. Since  $\lambda$  is also

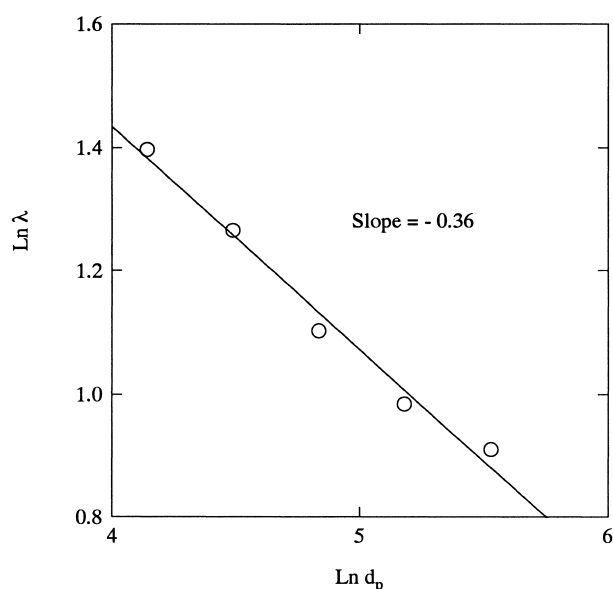


Fig. 3.  $\lambda$  vs. particle size ( $d_p$  in  $\mu\text{m}$ ).

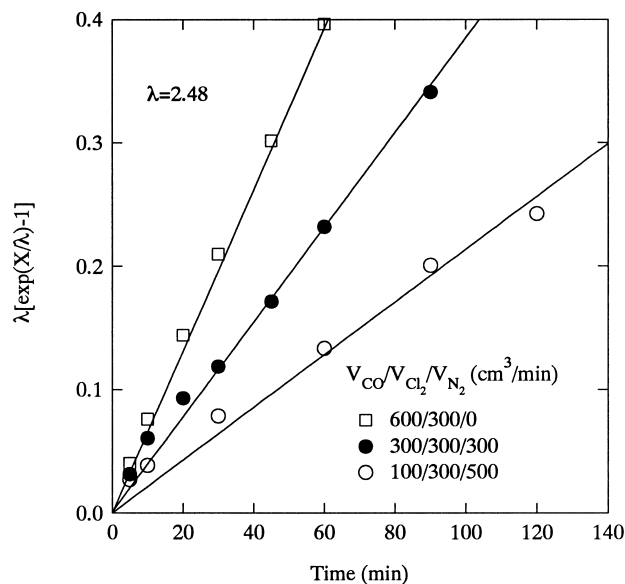


Fig. 4. Effect of CO partial pressure ( $T=900^\circ\text{C}$ ; flow rates at  $25^\circ\text{C}$  and  $86.1 \text{ kPa}$ ).

dependent on temperature, the complete expression of  $\lambda$  will be discussed subsequently.

### 3.3. Effect of partial pressures of reactant gases

Experiments were carried out with various mixtures of carbon monoxide and chlorine gases to investigate the effects of their partial pressures on the reaction rate. The chlorination temperature was  $900^\circ\text{C}$ . The particle size of beneficiated ilmenite was  $150\text{--}212 \mu\text{m}$ . The different partial pressures of reactant gases were obtained by varying the corresponding flow rates of the gases and introducing nitrogen to keep the total flow rate of inlet gas at  $900 \text{ cm}^3/\text{min}$ . Three groups of experiments were made for each reactant gas with partial pressure changing from  $9.6$  to  $57 \text{ kPa}$ . The results are shown in Figs. 4 and 5, in which chlorine is observed to have greater influence on the chlorination rate than carbon monoxide. Similarly, the values of  $\lambda$ , which was a function of particle size and temperature but was found to be independent of gaseous reactant partial pressures, were obtained from experimental results with various conditions by using the curve fit program in Sigma Plot. The slopes yield the values of  $k_{\text{app}}$ .

Assuming that  $k_{\text{app}}$  has a power-law dependence on the gaseous reactant partial pressures, as observed previously for the chlorination of rutile [6–8],

$$k_{\text{app}} = k p_{\text{CO}}^m p_{\text{Cl}_2}^n \quad (4)$$

where  $m$  and  $n$  are constants to be determined, and  $k$  a constant at a fixed temperature.  $m$  was obtained from the slope of the plot for different partial pressures of carbon monoxide, holding the partial pressure of chlorine gas constant as shown in Fig. 6, and  $n$  was obtained the same

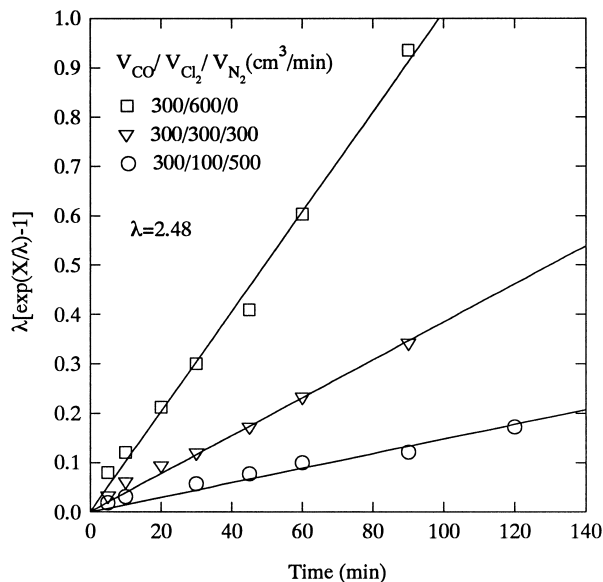


Fig. 5. Effect of  $\text{Cl}_2$  partial pressure ( $T=900^\circ\text{C}$ ; flow rates at  $25^\circ\text{C}$  and  $86.1\text{ kPa}$ ).

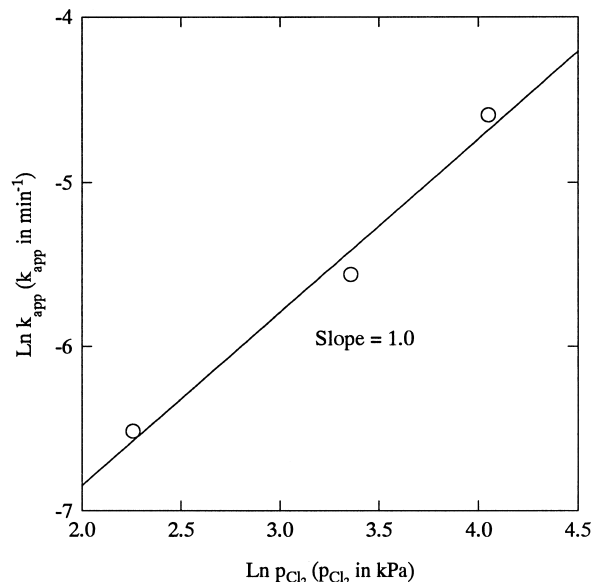


Fig. 7. Dependence of  $k_{\text{app}}$  on  $p_{\text{Cl}_2}$ .

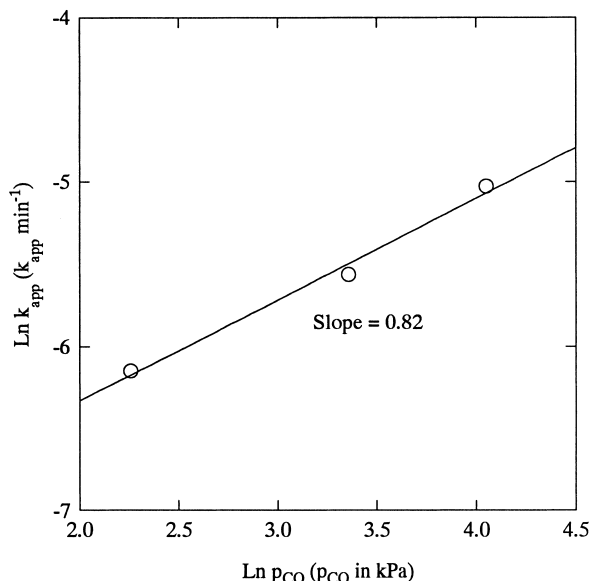


Fig. 6. Dependence of  $k_{\text{app}}$  on  $p_{\text{CO}}$ .

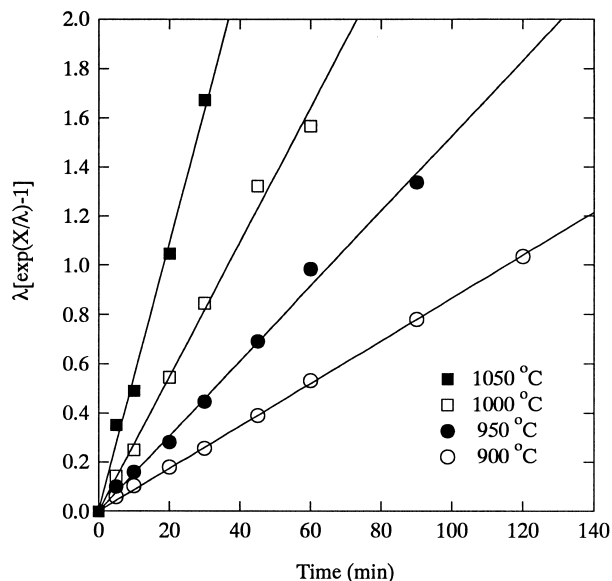


Fig. 8. Effect of temperature on the rate ( $p_{\text{CO}}=p_{\text{Cl}_2}=43\text{ kPa}$ ).

way, as shown in Fig. 7. The rate equation can now be written as:

$$\lambda[\exp(X/\lambda) - 1] - b = kp_{\text{CO}}^{0.82}p_{\text{Cl}_2}^{1.0}t \quad (5)$$

### 3.4. Effect of temperature

In order to determine the effect of temperature on the chlorination rate, experiments were performed in the  $900\text{--}1050^\circ\text{C}$  range at  $50^\circ\text{C}$  intervals. The partial pressures of both chlorine and carbon monoxide was kept at  $43\text{ kPa}$ . The initial particle size of beneficiated ilmenite was  $150\text{--}212\ \mu\text{m}$ . Fig. 8 shows the results, from which it can be seen that the chlorination rate increases significantly with

temperature. The appropriate  $\lambda$  values at different temperatures were also obtained from the curve fit program. The rate constant,  $k$ , can be obtained from the slopes in Fig. 8 and by applying Eq. (5). Fig. 9 shows the Arrhenius plot and best-fit straight line through the data. Therefore, considering all the parameters obtained above, the overall rate expression for the chlorination of beneficiated ilmenite can be represented by:

$$\lambda[\exp(X/\lambda) - 1] - b = 69.0 \exp(-18800/T)p_{\text{CO}}^{0.82}p_{\text{Cl}_2}^{1.0}t \quad (6)$$

where  $b$  has the expression given in Eq. (3), the apparent activation energy,  $E$ , equals  $156000\text{ J/mol}$ ,  $p_{\text{CO}}$  and are in  $\text{kPa}$ ,  $T$  in  $\text{K}$ , and  $t$  in  $\text{min}$ .

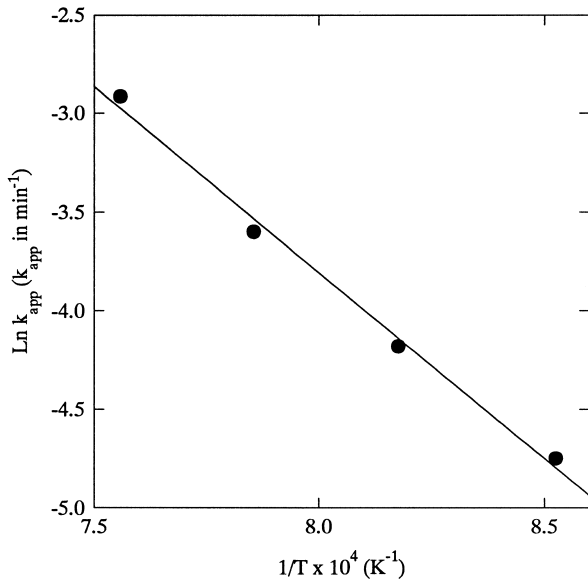


Fig. 9. Arrhenius plot of the rate constants.

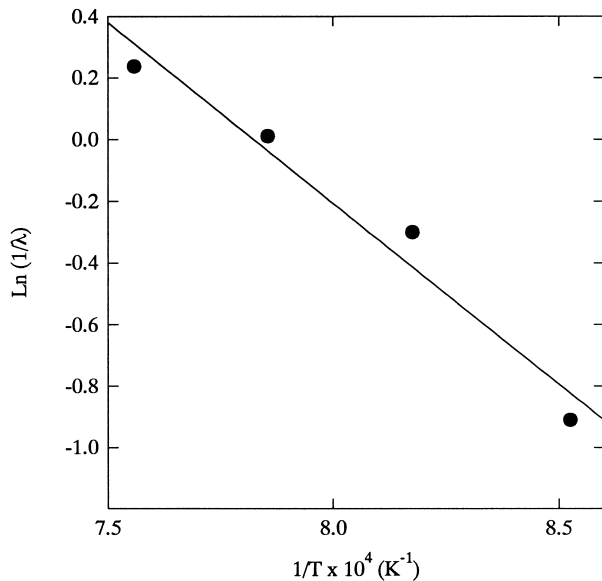


Fig. 10. Temperature dependence of  $1/\lambda$ .

The parameter  $\lambda$  varies with temperature, according to an Arrhenius-type relationship as shown in Fig. 10. Combining the effect of the original particle diameter,  $\lambda$  has the following expression:

$$1/\lambda = 1.32 \times 10^3 d_p^{0.36} \exp(-11700/T) \quad (7)$$

where  $d_p$  is in  $\mu\text{m}$  and  $T$  in K.

### 3.5. Comparison of beneficiated ilmenite and natural rutile chlorination

Beneficiated ilmenite chlorinated much faster than natural rutile. This is mainly due to the porous nature of the

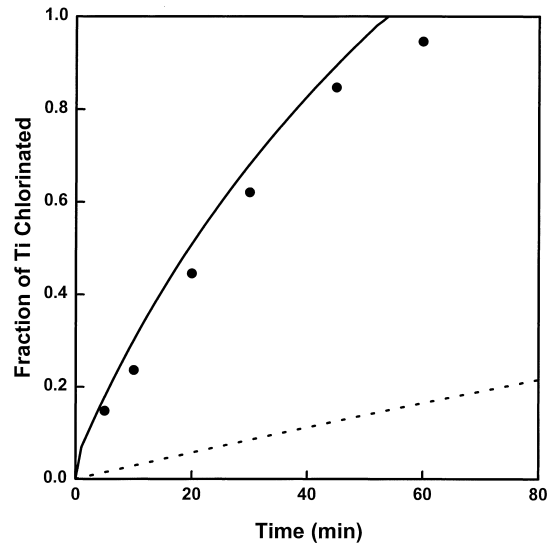


Fig. 11. Comparison of chlorination rate of beneficiated ilmenite concentrate (BIC) with that of rutile: (●) BIC, experimental; (—) BIC, calculated; and (---) Rutile ( $T=1000^\circ\text{C}$ ;  $p_{\text{CO}}=p_{\text{Cl}_2}=43 \text{ kPa}$ ;  $d_p=210\text{--}297 \mu\text{m}$ ).

former which provides a much larger specific surface area than the dense natural rutile [9]. A comparison was made using the foregoing rate expression and in the rutile chlorination study [6], as shown in Fig. 11. The apparent activation energies for the chlorination of beneficiated ilmenite and natural rutile are similar at 156 and 175 kJ/mol, respectively, which is expected, since in both cases the reaction involves the chlorination of titanium dioxide.

## 4. Concluding remarks

The chlorination of beneficiated ilmenite was studied in a shallow fluidized-bed reactor. The effects of various parameters on the chlorination rate were investigated. The pore-blocking rate law was found to yield the most satisfactory representation of the experimental data. Chlorine gas has a greater influence on the reaction rate than carbon monoxide, as in the case of natural rutile chlorination. Original particle size has a relatively small effect on the chlorination rate. The overall rate expression for the chlorination of beneficiated ilmenite was established as given in Eq. (6). Because of the limited resource of natural rutile, the beneficiated ilmenite will play an increasingly important role in the production of  $\text{TiCl}_4$ . The rate expression obtained here will provide useful information in the utilization of this material.

## 5. Nomenclature

- $b$  constant in Eqs. (3), (5) and (6) (—)
- $d_p$  particle size ( $\mu\text{m}$ )
- $k$  reaction-rate constant ( $\text{kPa}^{-1.82} \text{ s}^{-1}$ )
- $k_{app}$  apparent reaction-rate constant ( $\text{kPa}^{-1.82} \text{ s}^{-1}$ )

$p$	partial pressure (kPa)
$t$	time (min)
$T$	temperature (K)
$X$	fractional conversion (–)
$\lambda$	pore blockage constant (–)

### Acknowledgements

This work was supported in part by Du Pont's Chemicals and Pigments Department through an unrestricted research grant to the University of Utah. Special thanks go to Drs. Gary K. Whiting, Peter C. Compo, and Kevin J. Leary of Du Pont for helpful technical discussions and support. One of the authors (L. Zhou) received during the course of this work a Graduate Fellowship from Utah MRRRI and a University of Utah Graduate Research Fellowship.

### References

- [1] F.H. Hayes, H.B. Bomberger, F.H. Froes, L. Kaefman, H.L. Burtes, *JOM* 36(6) (1984) 70–75.
- [2] N.H. Orr, *Light Metals*, TMS, Warrendale, PA, 1982, pp. 1149–1156.
- [3] R. Powell, *Titanium Oxide and Titanium Tetrachloride*, Noyes Devel. Co., New York, 1968, pp. 1–6.
- [4] P.C. Turner, J.F. Hensen, *Adv. Mater. Proc.* 143(1) (1993) 42–43.
- [5] O. Nado, *Light Metals*, TMS, Warrendale, PA, 1988, pp. 759–768.
- [6] H.Y. Sohn, L. Zhou, K. Cho, *Ind. Eng. Chem. Res.* 37 (1998) 3800–3805.
- [7] W.E. Dunn Jr., *Trans. AIME* 218 (1960) 6–12.
- [8] A.J. Morris, R.F. Jensen, *Metall. Trans. B* 7B (1976) 89–93.
- [9] L. Zhou, H.Y. Sohn, G.K. Whiting, K.J. Leary, *Ind. Eng. Chem. Res.* 35 (1996) 954–962.
- [10] L. Zhou, H.Y. Sohn, *AIChEJ.* 42 (1996) 3102–3112.
- [11] K.I. Rhee, H.Y. Sohn, *Metall. Trans. B* 21B (1990) 321–330.
- [12] K.I. Rhee, H.Y. Sohn, *Metall. Trans. B* 21B (1990) 331–340.
- [13] Jandel Scientific Inc, Sigmaplot, Corte Madera, CA, 1991.